Adsorption of a minority component in polymer blend interfaces

C. Huang[1] and M. Olvera de la Cruz[1,2]
[1]*Department of Materials Science and Engineering, Northwestern University, Evanston, Illinois 60208*
[2]*Commissariat à l'Energie Atomique, Service de Chimie Moléculaire, Centre d'Etudes Nucléaires de Saclay, 91191 Gif-sur-Yvette Cedex, France*
(Received 24 August 1995)

We analyze the adsorption per interfacial thickness of the minority component C, Γ_C, in the interfaces between A and B rich phases in ternary polymer blends as a function of $\bar{\varphi}_C < \bar{\varphi}_A = \bar{\varphi}_B$, where $\bar{\varphi}_I$ is the mean composition of I, and the net interaction per thermal energy between I and J, χ_{IJ}. We find Γ_C solving numerically the nonlinear decomposition equations in the steady state. When C is nonselective, $\chi_{AC}=\chi_{BC}=\eta\chi_{AB}$, Γ_C increases as η increases and it is linear with $\bar{\varphi}_C$ for $\bar{\varphi}_C \ll \bar{\varphi}_A+\bar{\varphi}_B$. For selective C, $\chi_{AC}=\eta\chi_{AB}$ and $\chi_{BC}=\varepsilon\chi_{AB}$, in the case of minimum adsorption, $\eta=0$, Γ_C decreases as ε increases and it vanishes when $\varepsilon \geq 1$.

PACS number(s): 05.70.Fh, 64.75.+g, 82.65.Dp, 64.60.−i

I. INTRODUCTION

For many years the polymer community has been dedicated to producing polymer alloys with improved properties. Since polymer blends are strongly incompatible, nonhomogeneous microstructures result upon mixing. The morphology, in particular the interfacial thickness and its composition, determines the mechanical properties of these multiple phase materials. Binary polymer blends are well understood [1]. Since limited interface modifications are possible, the addition of A-B copolymers to immiscible A and B polymers [2,3] has been proposed as a mechanism to alter the interfacial properties. A chemically inhomogeneous minority component, however, is not necessary to change the interfaces of immiscible A and B blends. Here we determine in which circumstances a chemically homogeneous polymer C segregates in the interfaces between α and β phases rich in A and B polymers, respectively.

The excess composition of C at the α and β interfaces is a function of the net interaction per thermal energy (k_BT) between components I and J, χ_{IJ}. In nonselective C systems with no interactions between A and C and B and C ($\chi_{AC}=\chi_{BC}=0$), one would expect that polymer C segregates in the interfaces between α and β phases since it decreases the contacts between A and B [4]. In this paper we analyze the adsorption of nonselective ($\chi_{AC}=\chi_{BC}=\eta\chi_{AB}$) and selective ($\chi_{AC}\neq\chi_{BC}=\varepsilon\chi_{AB}$) minority components C in the α and β interfaces as a function of $\bar{\varphi}_C < \bar{\varphi}_A = \bar{\varphi}_B$, where $\bar{\varphi}_I$ is the mean composition of I, and thermal energy (η and ε) in ternary blends with A, B, and C degrees of polymerization equal to N, $N_A=N_B=N_C=N$. This adsorption has a strong effect on the kinetics and the microstructures during phase separation in ternary mixtures [5].

Consider a ternary system described by the free energy functional per site,

$$\Delta f=\Delta f_0+\sum_{I=A,B,C}\bar{\kappa}_{II}(\nabla\varphi_I)^2 \tag{1}$$

where Δf_0 is the free energy per site of a homogeneous system, and $\bar{\kappa}_{II}$ is the gradient energy term coefficient reflecting the unfavorable nature of inhomogeneities. When Δf_0 is unstable, such that equilibrium is established if two phases coexist, the compositional gradient terms are required to determine the equilibrium interface profile. The adsorption of C in a flat interface can be determined from the equilibrium interface profile, given by the lowest minimum of the specific interfacial energy σ. In a flat interface between α and β of compositions $\bar{\varphi}_I^{\alpha}$ and $\bar{\varphi}_I^{\beta}$, σ is given by the difference per unit area of interface between the actual free energy and that which it will have if the properties of the two phases were continuous [6],

$$\sigma=N_V\int_{-\infty}^{\infty}\left[\Delta f_0^m+\sum_{I=A,B,C}\bar{\kappa}_{II}\left[\frac{d\varphi_I}{dx}\right]^2\right]dx\ , \tag{2}$$

where N_V is the number of monomers per unit volume and

$$\Delta f_0^m=\sum_{I=A,B,C}\frac{\varphi_I(x)}{N_I}[\mu_{0,I}(\{\varphi_I(x)\})-\mu_{0,I}(\{\bar{\varphi}_I^{\alpha}\})]\ , \tag{3}$$

where $\mu_{0,I}$ is the chemical potential of I in a homogeneous system. The composition of C is eliminated through the incompressibility constraint. Hence the specific interfacial energy σ in Eq. (2) can be rewritten as

$$\sigma=N_V\int_{-\infty}^{\infty}\left[\Delta f_0^m+\kappa_{AA}\left[\frac{d\varphi_A}{dx}\right]^2+2\kappa_{AB}\frac{d\varphi_A}{dx}\frac{d\varphi_B}{dx}+\kappa_{BB}\left[\frac{d\varphi_B}{dx}\right]^2\right]dx\ , \tag{2a}$$

with

$$\kappa_{II}=\bar{\kappa}_{II}+\bar{\kappa}_{CC},\quad I=A,B, \tag{4a}$$

$$\kappa_{AB}=\bar{\kappa}_{CC}\ . \tag{4b}$$

An extremum of $\sigma(\delta\sigma=0)$ is obtained solving simul-

taneously the resulting two Euler-Lagrange equations [7], which using the boundary conditions, Δf_0^m and $d\varphi_I/dx$ tend to zero as $x \to \pm\infty$ leads to

$$\Delta f_0^m = \kappa_{AA}\left[\frac{d\varphi_A}{dx}\right]^2 + 2\kappa_{AB}\frac{d\varphi_A}{dx}\frac{d\varphi_B}{dx} + \kappa_{BB}\left[\frac{d\varphi_B}{dx}\right]^2 . \tag{5}$$

There are many solutions for Eq. (5), and the actual minimum of σ cannot be obtained analytically [4]. The linearized solution for a flat α and β interface along the x axis, however, gives for a nonselective minority C ($\bar{\varphi}_C^\alpha = \bar{\varphi}_C^\beta = \bar{\varphi}_C$) values of $\varphi_C(x) - \bar{\varphi}_C > 0$, demonstrating the adsorption of C in the interface. The adsorption of a homopolymer in the interfaces of two segregated solvents ($N_A = N_B = 1$) has been studied by this method in Ref. [8]. Also, the linearized solution for the interfaces of a compressible binary blend (which corresponds to an athermal $\chi_{AC} = \chi_{BC} = 0$ minority solvent $N_C = 1$) shows an excess of vacancies at the interfaces. The linearized solution of Eq. (5) for ternary polymer blends will be given elsewhere.

In this paper we follow a different method to determine the interface profile which is not restricted to small $\varphi_C(x) - \bar{\varphi}_C$ values, and from this interface profile we compute the adsorption of C at the interfaces. We numerically solve the equilibrium composition profile $\varphi_I(x)$, $I = A$, B, and C, from the steady state solution of the nonlinear decomposition equations. In Sec. II the dynamical model and the techniques for numerically solving the nonlinear decomposition equations are described. The numerical results of the adsorption of C per interfacial thickness as a function of $\bar{\varphi}_C$ and thermal energy in nonselective and selective minority C systems are given in Secs. III and IV, respectively. In Sec. V we conclude and discuss our studies.

II. DYNAMICAL MODEL AND NUMERICAL METHODS

The kinetics of spinodal decompositions are described by the continuity equations [9],

$$\frac{\partial \varphi_I}{\partial t} = -\nabla \tilde{J}_I \quad I = A, B, C , \tag{6}$$

where the flux $\tilde{J}_I$ is chosen to obey the mass conservation $\sum_{I=A,B,C} \tilde{J}_I = 0$. In this reference frame for the flux, one finds $\tilde{J}_I = J_I - \varphi_I \sum_{I=A,B,C} J_I$ with $J_I = -M_I \nabla \mu_I^S$, $I = A$, B, and C, where μ_I^S, the chemical potential of I per site in an inhomogeneous system, is given by $\mu_I^S = \partial \Delta f_0 / \partial \varphi_I - 2\bar{\kappa}_{II}\nabla^2 \varphi_I$, and M_I is the Onsager coefficient of I. Eliminating the variable $\varphi_C(r,t)$ with the incompressibility condition and using the Gibbs-Duhem relationship $\sum_{I=A,B,C} \bar{\varphi}_I d\mu_I^S = 0$ locally, Eqs. (6) become

$$\frac{\partial}{\partial t}[\varphi_I(r,t)] = M_{II}\nabla^2(\mu_{0,I}^s - \mu_{0,C}^s - 2\kappa_{II}\nabla^2\varphi_I - 2\kappa_{IJ}\nabla^2\varphi_J) + M_{IJ}\nabla^2(\mu_{0,J}^s - \mu_{0,C}^s - 2\kappa_{JI}\nabla^2\varphi_I - 2\kappa_{JJ}\nabla^2\varphi_J), \quad I \neq J; I, J = A, B \tag{7}$$

where

$$\mu_{0,I}^s = \frac{\partial 0 f_0}{\partial \varphi_I}, \quad M_{II} = (1-\bar{\varphi}_I)^2 M_I + \varphi_I^2 \sum_{J\neq 1,\ J=A,B,C} M_J, \quad I = A, B,$$

and

$$M_{AB} = -(1-\bar{\varphi}_A)\bar{\varphi}_B M_A - (1-\bar{\varphi}_B)\bar{\varphi}_A M_B + \bar{\varphi}_A \bar{\varphi}_B M_C .$$

Since long polymer blends are well described by mean field theories, analytic forms of $\mu_{0,I}^s$ in Eqs. (7) can be used. Here for simplicity we use the Flory-Huggins mean field free energy per lattice site, or the regular solution model for blends, given by

$$\frac{\Delta f_0}{k_B T} = \frac{\varphi_A \ln \varphi_A}{N_A} + \frac{\varphi_B \ln \varphi_B}{N_B} + \frac{\varphi_C \ln \varphi_C}{N_C} + \chi_{AB}\varphi_A\varphi_B + \varphi_{BC}\varphi_B\varphi_C + \chi_{AC}\varphi_A\varphi_C . \tag{8}$$

The gradient energy terms are computed using the random phase approximation [10]

$$\bar{\kappa}_{II} = k_B T a^2/(36\bar{\varphi}_I), \quad I = A, B, C , \tag{9}$$

where a is the monomer size. More general approaches which lead to $\bar{\kappa}_{II}$ dependent on the local composition [11] [replacing $\bar{\varphi}_I$ is Eqs. (9) by $\varphi_I(r)$] do not affect our results. The mobility in blends of long degrees of polymerization is given by [12] $M_I = (\bar{\varphi}_I/N_I)(D_0 N_e/k_B T)$, where D_0 is the diffusion coefficient of monomers, and N_e is the effective number of monomers per entanglement length.

We solve Eqs. (7) in terms of dimensionless parameters $x = (k_B T/2\kappa N)^{1/2} r$ and $\tau = M(k_B T)^2 t/2\kappa N^2$, and reduced $m_{IJ} = M_{IJ}/M$ and $\tilde{\kappa}_{IJ} = \kappa_{IJ}/\kappa$, where $M = (1/4N)(D_0 N_e/k_B T)$ and $\kappa = k_B T a^2/9$. Equations (7) in dimensionless forms are solved using the finite-difference method for the spatial and the temporal derivatives. The values of Δx and $\Delta\tau$ are chosen to simulate continuous dynamics avoiding artificial numerical slowing down effects or pinning, due to the inability of Eqs. (7) to describe the kinetics of phase separation when the interfacial thickness is smaller than Δx. The simulations are done in a 2D square lattice with L^2 grids, with $L = 64$. Periodic boundary conditions are used to avoid surface effects. Since the initial high temperature state is a homogeneous mixture, the initial compositions φ_A and φ_B for each grid are chosen to be uniformly random number distributed in the interval $[\bar{\varphi}_A - \zeta, \bar{\varphi}_A + \zeta]$ and $[\bar{\varphi}_B - \zeta, \bar{\varphi}_B + \zeta]$, respectively. We choose $\zeta = 0.005$, $\Delta\tau = 0.01$, and $\Delta x = 1.2$ here. We have run the numerical simulation until the steady state is achieved. The steady state is achieved when the volume fractions and the com-

positions of the two phases reach the equilibrium values, and the dynamic structure factors are self-similar.

III. ADSORPTION OF C IN NONSELECTIVE MINORITY $C(\chi_{AC}=\chi_{BC}=\eta\chi_{AB})$ SYSTEMS

In the presence of a nonselective minority C, the adsorption of C per interfacial thickness in the α and β interfaces, Γ_C, in three dimensions is defined as

$$\Gamma_C=\frac{1}{\bar{V}}\int_V[\varphi_C(r)-\bar{\varphi}_C^e]dV\ , \tag{10}$$

where $\varphi_C^e=\bar{\varphi}_C^\alpha=\bar{\varphi}_C^\beta$, V is the volume of the whole system, and $\bar{V}$ is the volume of the interface. In two dimensions (2D) we substitute $V\rightarrow A, \bar{V}\rightarrow\bar{A}$, where A is the

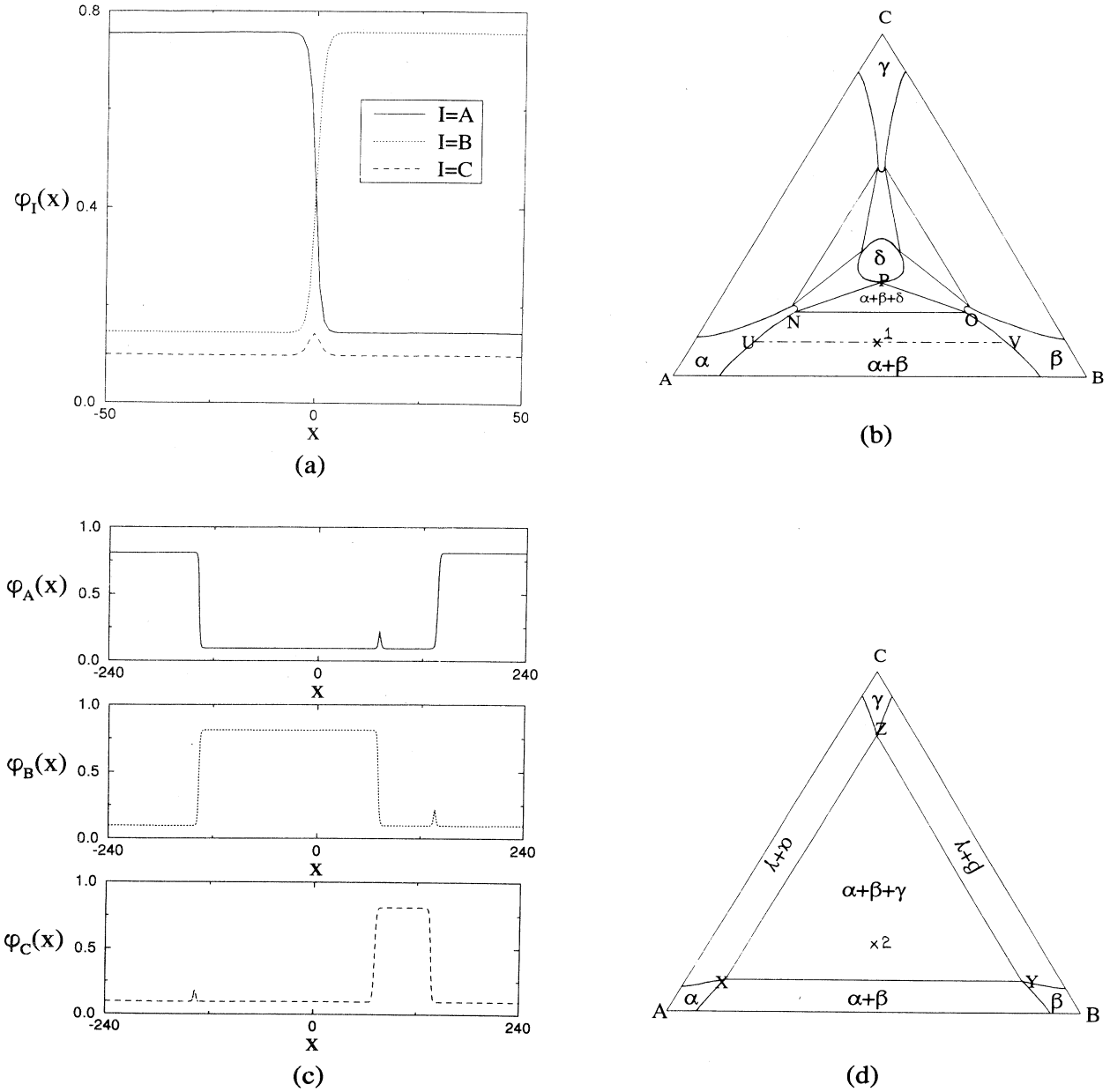

FIG. 1. The steady state composition profiles (a) and (c) for the symmetric ternary systems 1 shown in (b) and 2 shown in (d), with mean compositions (0.45,0.45,0.1) and (0.4,0.4,0.2), respectively. The phase diagrams for (b) $\chi N=2.7$ and (d) $\chi N=3.0$. In (b) the equilibrium compositions in the tie line (—— · ——) are given by $U=(0.754,0.146,0.1)$ for α, and $V=(0.146,0.754,0.1)$ for β, respectively, and in (d) the equilibrium compositions, $X=(0.811,0.0945,0.0945)$ for α, $Y=(0.0945,0.811,0.0945)$ for β, and $Z=(0.0945,0.0945,0.811)$ for γ, respectively. Plots of (e) $\langle R\rangle_{AA}$ vs $\tau^{1/3}$ and (f) $S_{AA}(k,\tau)/\langle R\rangle_{AA}^2$ vs $k\langle R\rangle_{AA}$ of system 1. The scaling results shown in (f) are valid from $\tau=7600$. $S_{AA}(k,\tau)$ is defined as $\sum_{|\mathbf{k}|=k}S_{AA}(\mathbf{k},\tau)/\sum_{|\mathbf{k}|=k}1$ with $S_{AA}(\mathbf{k},\tau)=\langle(1/L^2)\sum_{\mathbf{r}}\sum_{\mathbf{r}'}e^{i\mathbf{k}\cdot\mathbf{r}}[\varphi_A(\mathbf{r}+\mathbf{r}')\varphi_A(\mathbf{r}')-\bar{\varphi}_A^2]\rangle$, where the sums are over all of the L^2 grids, and $\mathbf{k}$ is the wave vector which belongs to the first Brillouin zone in reciprocal space. $\langle R\rangle_{AA}$ is defined as $1/\langle k\rangle_{AA}$ with $\langle k\rangle_{AA}=\sum kS_{AA}(k,\tau)/\sum S_{AA}(k,\tau)$.

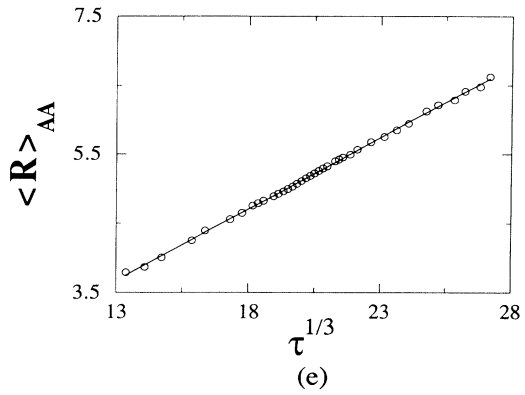

(e)

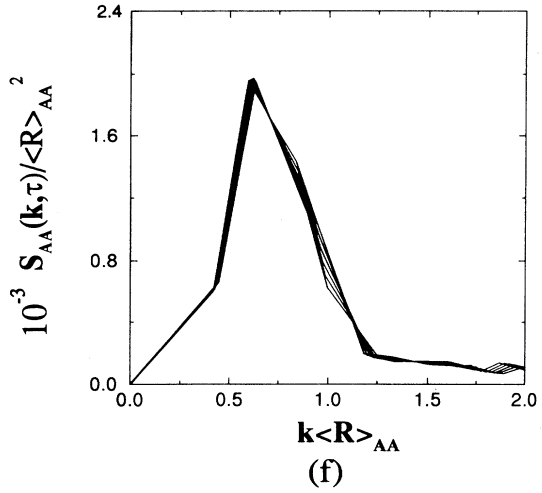

(f)

FIG. 1. (*Continued*).

area of the whole system and $\overline{A}$ is the area of the interface. According to Eq. (10), Γ_C is dimensionless and gives the excess compositions of C at the interfaces.

The steady state profile for blends with $\chi_{AB}=\chi_{AC}=\chi_{BC}=\chi$ and mean compositions $(\overline{\varphi}_A,\overline{\varphi}_B,\overline{\varphi}_C)=(0.45,0.45,0.10)$ at $\chi N=2.7$ is shown in Fig. 1(a). The equilibrium compositions $\overline{\varphi}_I^{\alpha}$ and $\overline{\varphi}_I^{\beta}$, $I=A$, B, and C, obtained by equating the chemical potential of each component, are given by the tie-line in the equilibrium ternary phase diagram shown in Fig. 1(b). In these blends we find $\Gamma_C\sim\overline{\varphi}_C$ for quenches deep into the two α and β phases. This scaling holds for systems undergoing two phase separation quenched far from critical points, and for deeper quenches where three phase regions appear in ternary phase diagrams.

Since the adsorption of a third component K in the interface between any two phases rich in I and J is a general phenomenon, it is also observed in quenches into three phase regions α, β, and γ, rich in A, B, and C, respectively. This is shown in the steady state composition profile for a system with initial compositions (0.4,0.4,0.2) at $\chi N=3.0$ in Fig. 1(c), which α, β, and γ phase equilibrium compositions are given by the corners of the XYZ triangle in the ternary phase diagram shown in Fig. 1(d). This adsorption strongly influences the microstructures during phase separation. Since the decomposition into three phases is initiated by decomposing into two phases α and β rich in A and B, respectively, and the minority component is adsorbed in the α and β interfaces during the decomposition, a third phase γ rich in the minority component will form at these interfaces. When the interface is very broad [as in quenches inside the small three-phase triangle NOP in Fig. 1(b)], the minority phase does not coarsen, it can be considered simply as increasing the interfacial thickness between the two majority phases. When the thermal energy decreases [as inside the triangle XYZ in Fig. 1(d)], the minority phase can no longer be considered to thicken the interface, but appears as a phase that separates these two majority phases in the later stages of the decomposition process.

In the absence of hydrodynamics we find that the growth law $R(\tau)\sim\tau^{1/3}$ is always obeyed in ternary systems undergoing two and three-phase separations even when the decomposition patterns are not self-similar. Ternary systems, however, do reach a scaling regime at the very late stages. Our dynamical scaling results are in agreement with the results obtained by Monte Carlo simulation [13] and molecular dynamics [14] in small molecule systems, where only the composition $\overline{\varphi}_I=\frac{1}{3}$, $I=A$, B, and C, was studied. In Fig. 1(e) we plot the domain growth as a function of time for a system with mean compositions (0.45, 0.45, 0.1) quenched to $\chi N=2.7$, showing the $\tau^{1/3}$ power law. In ternary systems the segregation of the minority component at the interfaces breaks the self-similarity observed even at the early stages of the decomposition in binary systems. Self-similarity, however, is obtained when the interface segregation reaches the steady state [see Fig. 1(f)]. A thorough analysis of the scaling of the phase separation dynamics is given elsewhere [5].

The adsorption of a nonselective minority C, $\chi_{AC}=\chi_{BC}=\eta\chi_{AB}$, is at a minimum when $\eta=0$, and it increases as η increases. For example the adsorption of C calculated numerically from Eq. (10) in 2D for a system with initial compositions (0.45, 0.45, 0.1) at $\chi_{AB}N=2.7$ is 0.0067 for $\eta=0$, and 0.0117, more than 10% of $\overline{\varphi}_C$, for $\eta=1$. The steady state composition profile for the system with $\eta=0$ is shown in Fig. 2(a) and the equilibrium compositions of α and β are obtained by the tie-line in the ternary equilibrium phase diagram shown in Fig. 2(b). Our results can be understood analyzing the contribution to the free energy from infinitesimal compositional fluctuations. A Taylor's series expansion of Δf in the Fourier components of $\psi_1(r)=[\delta\varphi_A(r)-\delta\varphi_B(r)]/(2\overline{\varphi})$ and $\psi_2(r)=-\delta\varphi_C(r)$, where $\overline{\varphi}=\overline{\varphi}_A+\overline{\varphi}_B$, and $\delta\varphi_I(r)=\varphi_I(r)-\overline{\varphi}_I$, $I=A$, B, and C, in systems with $\overline{\varphi}_A=\overline{\varphi}_B$, is given by

$$\Delta f(\{\psi_1(k),\psi_2(k)\}) \sim \sum_{I=1,2}\sum_{k}\frac{\Omega_{II}(k)}{2}\psi_I^2(k)+\sum_{k,k',k''}\frac{\Omega_{112}}{3!}\delta(k+k'+k'')\psi_1(k)\psi_1(k')\psi_2(k'') + \sum_{k,k',k'',k'''}\frac{\Omega_{1111}}{4!}\delta(k+k'+k''+k''')\psi_1(k)\psi_1(k')\psi_1(k'')\psi_1(k''') , \quad (11)$$

where

$$\Omega_{11}(k)=\bar{\varphi}^2[4/(\bar{\varphi}N)-2\chi_{AB}+4\bar{\kappa}_{AA}k^2] , \quad (12a)$$

$$\Omega_{22}(k)=1/[\bar{\varphi}(1-\bar{\varphi})N]+(0.5-2\eta)\chi_{AB}+(\bar{\kappa}_{AA}+2\bar{\kappa}_{CC})k^2 , \quad (12b)$$

$$\Omega_{112}=-12/N , \quad (12c)$$

$$\Omega_{1111}=32\bar{\varphi}/N . \quad (12d)$$

For a single wave compositional fluctuation of wavelength $\lambda_1=2\pi/k_1$, $\psi_1(r)=A_1e^{i\mathbf{k}_1\cdot\mathbf{r}}+\text{c.c.}$, if $\chi_{AB}N>2/\bar{\varphi}+2\bar{\kappa}_{AA}k_1^2$ a compositional fluctuation in $\psi_2(r)=A_2e^{i\mathbf{k}_2\cdot\mathbf{r}}+\text{c.c.}$ of half wavelength $k_2=2k_1$ is induced by the negative Ω_{112} term in Eq. (11). For this periodic pure interface profile between A and B, the composition of the minority C is maximum when $\delta\varphi_I(r)=0$, $I=A$ and B, which means it segregates at the interfaces. The

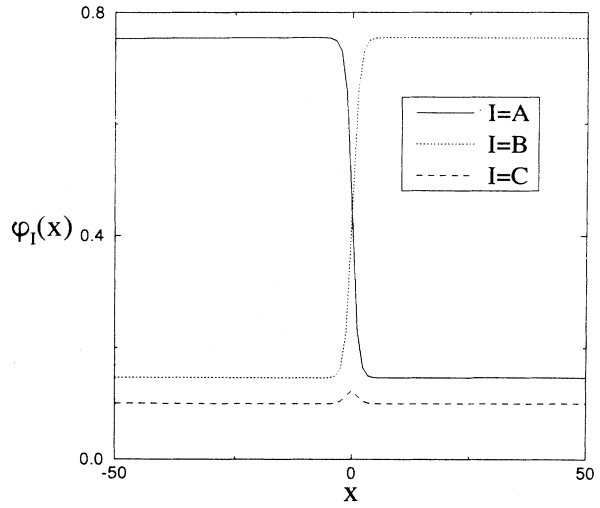

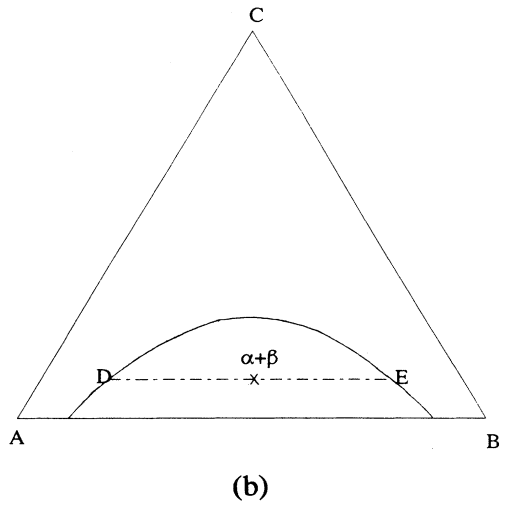

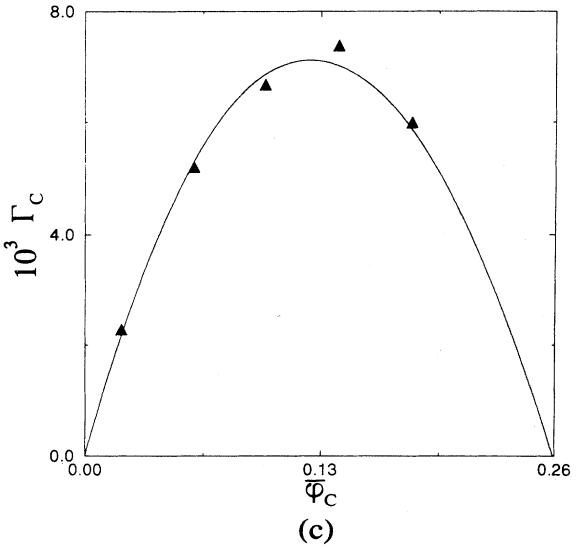

FIG. 2. (a) The steady state composition profile of a nonselective C system ($\chi_{AC}=\chi_{BC}=0$) with mean compositions (0.45, 0.45, 0.1) for $\chi_{AB}N=2.7$, shown as (x) in the phase diagram (b), in which the equilibrium compositions in the tie line (——·——), $D=(0.754,0.146,0.1)$ for α, and $E=(0.146,0.754,0.1)$ for β, respectively. (c) Plot of Γ_C in Eq. (10) in 2D vs $\bar{\varphi}_C$ in systems with $\bar{\varphi}_A=\bar{\varphi}_B$. The solid curve is obtained calculating $\bar{A}_2$ in Eq. (13) multiplied by a constant 0.23.

most probable amplitude of the induced compositional fluctuation in C, $\overline{A}_2$, is given by

$$\overline{A}_2=\frac{\Omega_{11}(k_1)\Omega_{112}}{\Omega_{1111}\Omega_{22}(k_2)-\Omega_{112}^2/3}\ , \tag{13}$$

and as η increases $\overline{A}_2$ increases. When $\eta\chi_{AB}N$ increases such that $\Omega_{1111}\Omega_{22}(k_2=0)-\Omega_{112}^2/3<0$, however, three phases will appear in the steady state. In this case there is adsorption of each component for deep quenches as shown for the symmetric case $\eta=1$ at $\chi_{IJ}N=\chi N=3$ in Fig. 1(c).

Though Eqs. (11)–(13) cannot be used to describe deep quenches in the steady state when the compositional fluctuations are not small (also we must include mass conservation laws), it suggests that Γ_C in Eq. (10), proportional to $\overline{A}_2$, is indeed linear in $\overline{\varphi}_C$ for $\overline{\varphi}_C \ll \overline{\varphi}$. When $\eta\chi_{AB}N$ is small, however, a critical point appears when $\overline{\varphi}_C$ increases towards $\overline{\varphi}_C^{\rm crit}=1-2/(\chi_{AB}N)$, shown in Fig. 2(b) for $\eta=0$, and the adsorption of C should decrease as $\overline{\varphi}_C$ increases, $\overline{A}_2(k_1=0)\sim\overline{\varphi}_C(1-\overline{\varphi}_C)(\overline{\varphi}_C^{\rm crit}-\overline{\varphi}_C)$. This suggests a maximum of the adsorption at a certain $\overline{\varphi}_C<\overline{\varphi}_C^{\rm crit}$. The numerical results for the adsorption when $\eta=0$ are shown in Fig. 2(c). In this figure we compare the adsorption computed from the values of $\overline{A}_2(k_1=0)$ in Eq. (13) multiplied by a constant with the numerical results in the steady state. They are in good agreement, though the adsorption of C per interfacial thickness near the critical point cannot be obtained from our equations because the effects of the heat bath terms are neglected (also, mean field results do not hold near critical points).

IV. ADSORPTION OF C IN SELECTIVE MINORITY $C(\chi_{AC}=\eta\chi_{AB};\chi_{BC}=\varepsilon\chi_{AB})$ SYSTEMS

The adsorption in systems with a selective minority component C, $\chi_{BC}=\varepsilon\chi_{AB}$, is analyzed for simplicity setting $\chi_{AC}=0$. When C is selective ($\varepsilon\neq 0$) the equilibrium composition of C in the α and β phases is not equal. In Fig. 3(a) we show the interface composition profile in the steady state for a system of initial compositions (0.45, 0.45, 0.1) at $\chi_{AB}N=2.7$ and $\varepsilon=0.2$. The equilibrium compositions $\overline{\varphi}_I^{\alpha}$ and $\overline{\varphi}_I^{\beta}$ are obtained by the tie-line in the phase diagram shown in Fig. 3(b). When $\overline{\varphi}_C^{\alpha}\neq\overline{\varphi}_C^{\beta}$, the adsorption of component I per interfacial thickness, Γ_I, is defined as the excess composition of I in an ideal system consisting of α and β phases assumed homogeneous right up to a dividing surface Σ, in 3D:

$$\Gamma_I=\frac{I}{\overline{V}}\left[\int_V\varphi_I(r)dV-V^{\alpha}\overline{\varphi}_I^{\alpha}-(V-V^{\alpha})\overline{\varphi}_I^{\beta}\right]\ , \tag{14}$$

where V^{α} is the volume of α phase in the ideal system. In 2D, $V\to A$, $\overline{V}\to\overline{A}$, and $V^{\alpha}=A^{\alpha}$, where A^{α} is the area of the α phase in the ideal system. Even though for selective minority component systems Γ_I depends on the position Σ, $\Gamma_J^{(I)}$ defined as

$$\Gamma_J^{(I)}=\Gamma_J-\Gamma_I\frac{\overline{\varphi}_J^{\alpha}-\overline{\varphi}_J^{\beta}}{\overline{\varphi}_I^{\alpha}-\overline{\varphi}_I^{\beta}},\quad J\neq I \tag{15}$$

is independent of the position of Σ. Therefore we analyze the adsorption of C, per interfacial thickness in selective C systems in terms of $\Gamma_C^{(A)}=\Gamma_C^{(B)}=\overline{\Gamma}_C$ in Eq. (15). Notice that $\varepsilon=1$ corresponds to a binary blend with $\overline{\varphi}_1=\overline{\varphi}_B$ and $\overline{\varphi}_2=\overline{\varphi}_A+\overline{\varphi}_C$, therefore there is no adsorption. Furthermore, for any value of $\varepsilon>1$ we find no adsorption of C and the maximum adsorption is for $\varepsilon=0$, the nonselective case of minimum adsorption ($\eta=0$). The numerical results of $\overline{\Gamma}_C$ with $\overline{\varphi}_C$ and ε for systems with $\overline{\varphi}_A=\overline{\varphi}_B$ are given in Fig. 4(a). In this figure we only show quenches far away from critical points, where we find that as φ_C increases $\overline{\Gamma}_C$ increases.

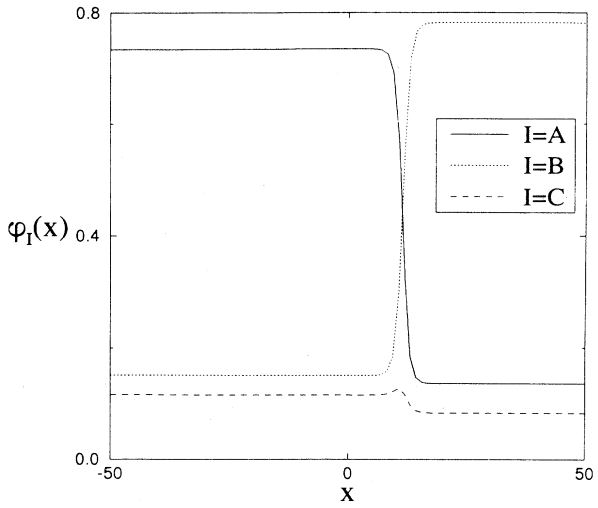

(a)

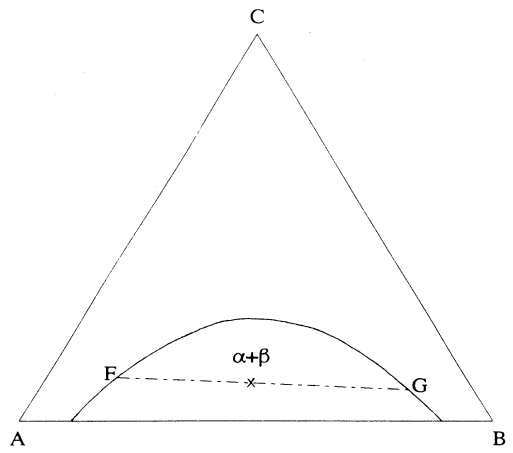

(b)

FIG. 3. (a) The steady state composition profile of a selective C system ($\chi_{AC}=0$, $\chi_{BC}=0.2\chi_{AB}$) with mean compositions (0.45,0.45,0.1) for $\chi_{AB}N=2.7$, shown as (x) in the phase diagram (b), in which the equilibrium compositions in the tie line (——·——), $F=(0.734,0.151,0.115)$ for α, and $G=(0.135,0.782,0.083)$ for β, respectively.

Since the adsorption of C defined in Eq. (15) is related to $\Delta\varphi_1^e = |\bar{\varphi}_I^\alpha - \bar{\varphi}_I^\beta|$, we analyze $\Delta\varphi_I^e$, $I = A$, B, and C, as a function of $\bar{\varphi}_C$ and ε. The equilibrium compositions are obtained by equating the chemical potential of each component. We find $\Delta\varphi_C^e \sim \bar{\varphi}_C^b$, where $b \cong 0.945$ for $\bar{\varphi}_C \ll \bar{\varphi}_A + \bar{\varphi}_B$ and $\Delta\varphi_C^e/\bar{\varphi}_C^b$ is a universal scaling of ε, shown in Fig. 4(b), regardless of the values of $\bar{\varphi}_I$, $I = A$ and B (even for $\bar{\varphi}_A \neq \bar{\varphi}_B$). For $\varepsilon > 1$, when there is no adsorption, $\Delta\varphi_C^e/\bar{\varphi}_C^b$ is a universal scaling of ε for all $\bar{\varphi}_C$ values. Since the relations between $\Delta\varphi_I^e$, $I = A$, and B, with $\bar{\varphi}_C$ are not universal in the regime studied here ($\varepsilon < 1$), we could not find the scaling of $\bar{\Gamma}_C$ with $\bar{\varphi}_C$ and ε.

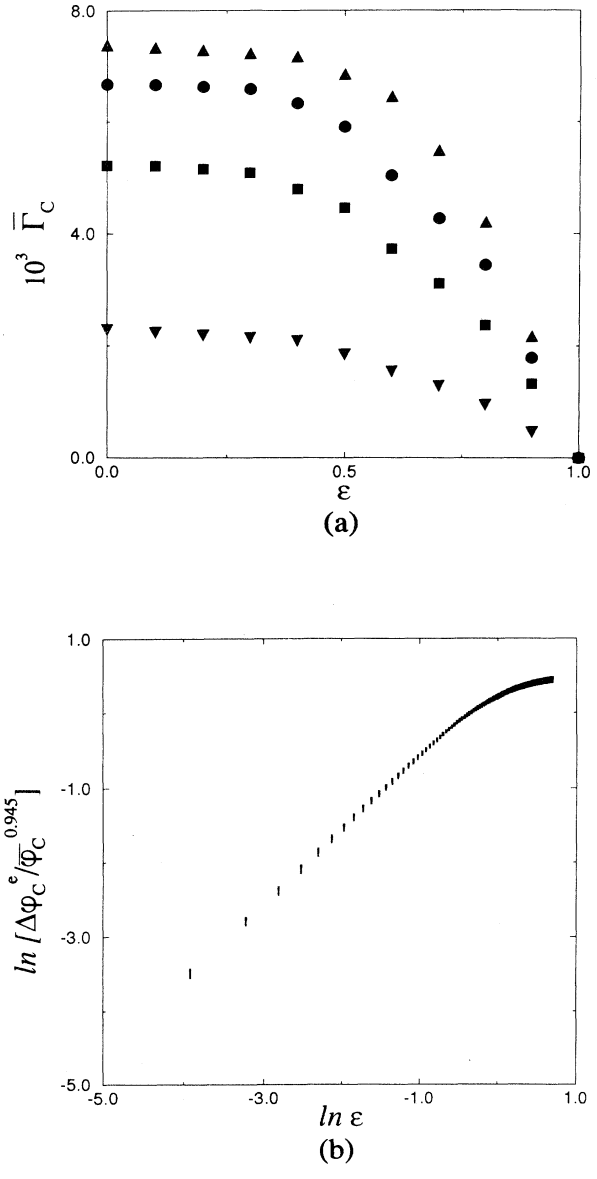

FIG. 4. In selective C systems ($\chi_{AC} = 0, \chi_{BC} = \varepsilon\chi_{AB}$) for $\chi_{AB}N = 2.7$: (a) Plot of $\bar{\Gamma}_C$ in Eq. (15) in 2D vs ε varying $\bar{\varphi}_C$ in systems with $\bar{\varphi}_A = \bar{\varphi}_B$. The symbols (▼), (■), (●), and (▲) correspond to $\bar{\varphi}_C = 0.02$, 0.06, 0.1, and 0.14, respectively. (b) Plot of $\ln(\Delta\varphi_C^e/\bar{\varphi}_C^{0.945})$ vs $\ln\varepsilon$ in the regime of $\bar{\varphi}_C \ll \bar{\varphi}_A + \bar{\varphi}_B$, and for $\varepsilon > 1$ regardless of $\bar{\varphi}_C$.

V. CONCLUSIONS AND DISCUSSION

We conclude that for nonselective minority component systems there are two types of behavior of the adsorption of the minority C: (1) when the system has a critical point increasing $\bar{\varphi}_C$, in which case there is a maximum in the adsorption of C per interfacial thickness, $\bar{\Gamma}_C$, at a certain $\bar{\varphi}_C < \bar{\varphi}_C^{\text{crit}}$; and (2) when there is a three-phase region increasing $\bar{\varphi}_C$, in which case there is adsorption of each component K in the interface between the I and J rich phases. In both cases, $\bar{\Gamma}_C \sim \bar{\varphi}_C$ for $\bar{\varphi}_C \ll \bar{\varphi}_A + \bar{\varphi}_B$ at deep enough quenches. In the deep quenches studied here the interfacial thickness is still much larger than the chains radius of gyration $R_g \propto N^{1/2}$, so the coarse grained free energy functional used here can describe the system.

For the general selective minority component systems where $\chi_{AC} = \eta\chi_{AB}$ and $\chi_{BC} = \varepsilon\chi_{AB}$, it is not possible to make scaling arguments due to the complex phase diagrams that result in these systems. However, one will always find adsorption in the two-phase region, provided η and ε are not too large. This is clear by the fact that we analyze the adsorption in the cases where there is the least amount of adsorption, $\eta = 0$ and $\varepsilon \neq 0$, shown in Fig. 4(a). In general, for systems with $\bar{\varphi}_C \ll \bar{\varphi}_A = \bar{\varphi}_B$ undergoing two-phase separation, the adsorption of C per interfacial thickness ($\bar{\Gamma}_C$) is symmetric about the line $\eta = \varepsilon$. As $\eta = \varepsilon$ increases, $\bar{\Gamma}_C$ increases. When ε (η) is fixed, $\bar{\Gamma}_C$ increases from $\eta = 0$ ($\varepsilon = 0$) up to $\eta = \varepsilon$, and then decreases as η (ε) increases.

Our results are in principle applicable to ternary mixtures of small molecules [we recover the linear dependence of Γ_C in Eq. (10) with $\bar{\varphi}_C$, setting $\bar{\kappa}_{II} = \kappa$ and $N_I = 1$ in our equations for deep quenches into the two- and three-phase regions]. When the range of interactions between the molecules is small, however, fluctuations will have large effects and the $2D$ results presented here will be at most qualitatively correct for deep quenches. Since in $3D$ polymer blends a molecule interacts with the $N^{1/2}$ molecules that are within the radius of gyration, mean field results are applicable, and our 2D results are therefore expected to reproduce the results in 3D.

The dynamics for deep quenches, such that the interfacial thickness is very narrow in the later stages of the decomposition, will be modified due to hydrodynamical effects [15]. Coarsening of the third phase rich in the minority component for deep quenches into the three-phase region, for example, will occur by the flow of material from one region to another. Since in our studies the volume fractions of the two phases rich in the majority components are equal, so that their interfaces are connected, the domain growth law of the minority phase will be very fast (a $R \sim \tau$ growth law is expected). The steady state interface profile obtained here, where the decomposition dynamics are driven by the interfacial gradients, however, will not be modified by the hydrodynamical

effects. Notice that for deep quenches into three phases the minority phase by both dynamic mechanisms grows at the junctions between the A-rich–B-rich interfaces (the critical nucleus forms at these junctions, and the flow material if hydrodynamics are present is from slender to thicker regions which are also at these junctions) giving the same pattern with different growth rates.

ACKNOWLEDGMENTS

We are indebted to Professor P. W. Voorhees for his many enlightening and helpful discussions. This work was supported by the National Science Foundation (PYI Grant No. DMR 9057764), the David and Lucile Packard Foundation, and the Ford Motor Co.

[1] E. Helfand and A. M. Sapse, J. Chem. Phys. **62**, 1327 (1975); H. Tang and K. F. Freed, *ibid.* **94**, 6307 (1991).
[2] K. R. Shull and E. J. Kramer, Macromolecules **23**, 4769 (1990); T. A. Vilgis and J. Noolandi, *ibid.* **23**, 2941 (1990).
[3] Y. Lyatskaya, D. Gersappe, and A. C. Balazs, Macromolecules **28**, 6278 (1995).
[4] M. Lifschitz and K. F. Freed, J. Chem. Phys. **98**, 8994 (1993).
[5] C. Huang, M. Olvera de la Cruz, and B. W. Swift, Macromolecules **28**, 7996 (1995).
[6] J. W. Cahn and J. E. Hilliard, J. Chem. Phys. **28**, 258 (1958).
[7] F. B. Hildebrand, *Methods of Applied Mathematics* (Prentice-Hall, New York, 1992).
[8] A. Halperin and P. Pincus, Macromolecules **19**, 79 (1986).
[9] E. J. Kramer, P. Green, and C. J. Palstrom, Polymer **25**, 473 (1984).
[10] P. G. de Gennes, J. Phys. (Paris) Lett. **40**, 69 (1979); K. Binder, J. Chem. Phys. **79**, 6387 (1983).
[11] H. Tang and K. F. Freed, J. Chem. Phys. **94**, 1572 (1991).
[12] P. G. de Gennes, J. Chem. Phys. **55**, 572 (1971).
[13] C. Jeppesen and O. G. Mouritsen, Phys. Rev. B **47**, 14 724 (1993).
[14] M. Laradji, O. G. Mouritsen, and S. Toxvaerd, Europhys. Lett. **28**, 157 (1994).
[15] L. P. McMaster, Adv. Chem. Series, **142**, 43 (1975); E. D. Siggia, Phys. Rev. A **20**, 595 (1979).